Available online at www.sciencedirect.com

SciVerse ScienceDirect

Ceramics International 39 (2013) 1111–1123

CERAMICS INTERNATIONAL

www.elsevier.com/locate/ceramint

The effect of the surface nanostructure and composition on the antiwear properties of zirconia–titania coatings

Ireneusz Piwoński*, Katarzyna Soliwoda, Aneta Kisielewska, Renata Stanecka-Badura, Kinga Kądzioła

University of Lodz, Department of Materials Technology and Chemistry, Pomorska 163, 90-236 Łódź, Poland

Received 14 March 2012; received in revised form 4 July 2012; accepted 6 July 2012
Available online 20 July 2012

Abstract

This study describes the preparation, surface imaging and tribological properties of titania coatings modified by zirconia nanoparticles agglomerated in the form of island-like structures on the titania surface. Titania coatings and titania coatings with embedded zirconia nanoparticles were prepared by the sol–gel spin coating process on silicon wafers. After deposition the coatings were heat-treated at 500 °C or 1000 °C. The natural tendency of nanoparticles to form agglomerates was used to build separated island-like structures unevenly distributed over the titania surface having the size of 1.0–1.2 μm. Surface characterization of coatings before and after frictional tests was performed by atomic force microscopy (AFM) and optical microscopy. Zirconia nanoparticles were imaged with the use of transmission electron microscopy (TEM). The tribological properties were evaluated with the use of microtribometer operating in ambient air at technical dry friction conditions under normal load of 80 mN. It was found that nanocomposite coatings exhibit lower coefficient of friction (CoF) and considerably lower wear compared to titania coating without nanoparticles. The lowering of CoF is about 40% for coatings heated at 500 °C and 33% for the coatings heated at 1000 °C. For nanocomposites the wear stability was enhanced by a factor of 100 as compared to pure titania coatings. We claim that enhanced tribological properties are closely related to the reduction of the real contact area, lowering of the adhesive forces in frictional contacts and increasing of the composite hardness. The changes in materials composition in frictional contact has secondary effect.

Keywords: B. Composites; C. Friction; D. TiO_2; D. ZrO_2

1. Introduction

The effective protection of fragile coatings against wear and mechanical damage can be provided with appropriate composition, structure, good adhesion to the surface, roughness and texture. One way to improve the tribological properties of materials is introducing nanosize particles in the material which substantially increase its fracture toughness, hardness and wear resistance [1–4]. It is known, that the state of the interface between coating and the covered substrate as well as strong bonding between dispersed particles to surrounding matrix considerably influence the mechanical properties of thin coatings. However, for strongly adhered coatings a crucial role in the improvement of antiwear properties and reducing friction under sliding conditions is played by the surface texturing. Therefore, in order to improve the tribological properties of the material, the formation of the surface texturing in the form of nanosize structures or patterns on the surface is highly desired. In this way the reduction of the contact area between two surfaces, lowering of the adhesion and friction can be obtained.

Nowadays, various techniques have been used for producing nano-textured materials, physical vapor deposition [5], chemical vapor deposition [6], dip-coating [7] and spin-coating [8], nanolithography techniques eg. electron-beam lithography [9], interference lithography [10] and imprint lithography [11].

Nair and Zou [12] reported a novel use of aluminum-induced crystallization (AIC) of amorphous silicon (a-Si) technique in nano-scale surface-texturing for tribological

*Corresponding author. Tel.: +48 42 635 58 33; fax: +48 42 635 58 32.
E-mail address: irek@uni.lodz.pl (I. Piwoński).

0272-8842/$ - see front matter © 2012 Elsevier Ltd and Techna Group S.r.l. All rights reserved.
http://dx.doi.org/10.1016/j.ceramint.2012.07.034

applications. It was found, by using scanning electron microscope (SEM) analysis, energy dispersive X-ray spectroscopy (EDS), X-ray diffraction (XRD), transmission electron microscope (TEM), and atomic force microscope (AFM), that various nano-textured samples were fabricated with poly-Si (111) grains as nano-textures. Authors showed that nano-textured poly-silicon crystallites significantly reduced the adhesion and friction forces compared to the smooth surface. It was also found, that not only texture height but also surface density of poly-silicon crystallites affect the adhesion and friction performances of the nano-textured samples.

Shafiei and Alpas [13] fabricated nanocrystalline textured films for low friction surfaces. The textured surface was inspired to lotus leaf using a cellulose acetate film, on which grains of Ni, having a size of about 30 nm, were electrodeposited. Some "Ni crowns" were also formed on the surface and their height was about 10 μm. It was found that this structures causes the reduction of the coefficient of friction measured for the textured surfaces (CoF = 0.16) compared to those measured for the smooth surfaces (CoF = 0.45). The reduction was caused by the differences in the contact area. For the textured surfaces the real contact area was smaller than for the non-textured surfaces. The Vickers microhardness of the films with textures was determined to be 4.42 GPa at load of 0.25 N.

Kustandi et al. [14] showed that texturized surfaces can reduce the coefficient of friction up to 35% compared to non-patterened surface. Moreover, reciprocating wear experiments revealed that the presence of textures on the polymer surface resulted in lower wear depth and width. The material transfer to the sliding surface was minimal.

Määttä et al. [15], by studying the tribological behavior of stainless steel under low sliding speeds and high contact pressures against different tool steels, reported that surface topography and surface roughness of the steel had a greater influence on the friction than steel composition.

Evaluation of the bending strength, fracture strain and Young's modulus and other parameters as a function of materials composition and sample preparation is presented in [16]. Investigated system consisting of Al_2O_3–TiO_2–ZrO_2 mixture was tested as a thin freestanding coatings. It was found that the addition of titania and zirconia to alumina increases the strength until a addition level of 15 wt%. As well, after heat treatment the sintering causes significant increase in strength. However, the precipitation of second phases can influence the strength in both directions. Results obtained in this paper were compared with results found in the literature obtained by other scientific groups.

Tribological properties of the sol–gel derived TiO_2–ZrO_2 thin films were investigated in the frictional couple with AISI 52100 steel and Si_3N_4 [17]. Recorded coefficient of friction values were low (0.14–0.20). The antiwear life of the titania–zirconia coatings was more than 5000 cycles under 0.5 N applied load. Excellent antiwear and friction reduction performance result from the microstructure of the coating which is dense, homogenous and consist of complete teragonal phase.

Detailed studies concerning the wear mechanisms of advanced ceramics such as Al_2O_3, Si_3N_4, SiC and ZrO_2 was presented by Kato and Adachi [18]. Mechanism of wear in various frictional contacts were described. In general two modes of wear can be distinguished: mild and sever wear. These modes depend on the mechanical and the thermal severity of contact. These studies exhibit the importance and potential of ceramic materials in tribological applications.

In this paper, two kinds of coatings have been studied. The first one is a thin, smooth titania coating. The second one is nanocomposite titania coating consisting of titania matrix with islands of commercial zirconia nanoparticles unevenly distributed on its surface. Both types of coatings were prepared using the sol–gel spin-coating method. Consequently, the tribological behavior of both systems is expected to be different. The aim of this work is to evidence such a difference by investigating the tribological properties of these materials.

2. Materials and methods

All coatings were deposited by the sol–gel spin-coating method with free evaporation at 1000 rpm on Si (100) silicon wafers. Coatings were dried at 100 °C for 2 h and then heat treated at 500 °C or 1000 °C for 2 h to obtain crystallization and densification.

2.1. Materials

Titanium (IV) ispopropoxide (TTIP) 98%—ABCR GmbH and Co. KG Karlsuhe, Germany.

Nanoparticles ZrO_2—AGH University of Science and Technology, Cracow, Poland.

Ethanol 99.8%—POCh, Chempur, Poland.

Isopropanol—2-propanol 99.7%, Chempur, Poland.

Si wafers (100)—Cemat Silicon S.A., Warsaw, Poland

2.2. Coatings preparation

Purely titania coatings and nanocomposite coatings were prepared using liquid sol or sol containing zirconia nanoparticles deposited by the spin-coating method on silicon Si (100) wafers at a speed of 1000 rpm. The procedure of sol preparation is based on hydrolysis of titanium (IV) isopropoxide $(C_3H_7O)_4Ti$ in isopropanol (i-C_3H_7OH) in air. The mixture was magnetically stirred for 1 h and next deposited on silicon wafers Si (100) by the spin-coating method. Prior to use Si wafers were washed in ethanol in ultrasonic bath. Nanocomposite titania coatings containing zirconia nanoparticles were prepared using the same procedure but the sol was stirred for 45 min. After that time, the proper amount of ZrO_2 nanoparticles (5–20 nm diameter) was added to the sol and resulted suspension was sonicated using ultrasonic gun (IKA

Labortechnik U200S, US-200-14, 14 mm, 105 W cm^{-1}, amplitude 50 μm). Final suspension was used to cover the Si (100) substrate by the spin-coating method. The molar ratio of PrOH:TTIP:ZrO_2 (nanoparticles) was 26:1:1.

The thickness of coatings was controlled by depositing 3, 6 or 10 drops of the liquid sol or suspension on the rotating substrate. Both types of coatings were dried at 100 °C and calcined at 500 °C or 1000 °C for 2 h in order to get anatase or rutile phase. The flow-chart of the preparing process of the titania coatings and composite coating is presented in Fig. 1. Detailed amounts of the compounds used in the preparation of titania coatings and titania-composite coatings are summarized in Table 1.

In the case of each coating the same preparation conditions were applied in order to get samples differing only in the surface texture resulting from the presence of zirconia nanoprarticles.

2.3. AFM measurements

The surface topography was imaged with the use of the commercial NT-MDT AFM equipped with a "Smena" head operating in air under ambient conditions in the tapping mode. Non-contact silicon cantilever covered by silicon nitride was used (MikroMasch, NSC35/Si_3N_4/AlBS) having spring constant $k=14$ N m^{-1} and the resonance frequency $\upsilon=260$ kHz.

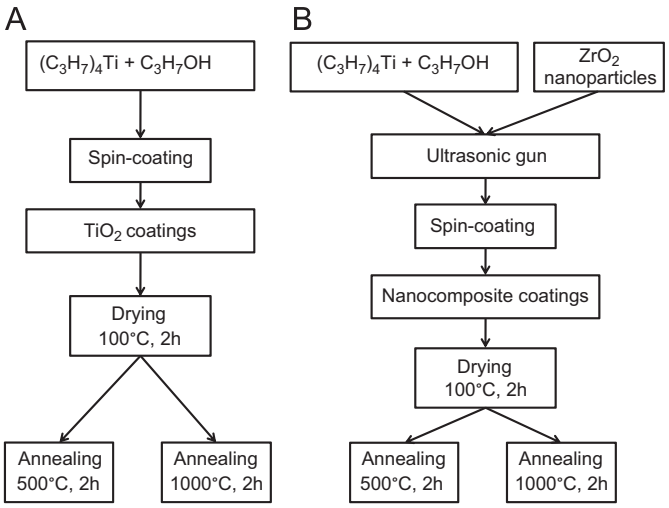

Fig. 1. Flow charts representing the process of titania coatings (A) and composite coatings containing nanoparticles (B) preparation.

Table 1
Detailed composition of the preparation bath of titania coatings and titania-composite coatings.

Compound	M (g mol^{-1})	n (mol)	d (g cm^{-3})	v (cm^3)	m (g)
$Ti(OC_3H_7)_4$	284.25	0.0050	0.963	1.484	1.429
PrOH	60.11	0.1306	0.785	10.000	7.850
np.* ZrO_2	123.22	0.0050	–	–	0.603

*Nanoparticles

2.4. SEM measurements

SEM imaging was performed on the VEGA 3 TESCAN equipment.

2.5. Film thickness measurements

Spectroscopic ellipsometer Horiba Jobin Yvon operating in the light wavelength 190–830 nm.

2.6. Tribological tests

Micro-scale friction tests were performed with a ball-on-flat type microtribometer (T-23) designed and constructed at the Department of Materials Technology and Chemistry, University of Lodz, Poland. The apparatus was dedicated particularly for tribological tests of ceramic, organic and composite thin films including sol–gel coatings. The microtribometer was equipped in two sensors recording normal and friction forces during sliding the ball over the investigated surface. Coefficients of friction were measured at the technical dry friction conditions. The applied normal load was 80 mN and the sliding speed was adjusted for 25 mm min^{-1}. Each test was repeated three times and the average values were plotted. The ceramic ball having the diameter 5 mm built of tetragonal zirconia polycrystals (TZP) stabilized with 3 mol% of Y_2O_3 was used as the counterbody in the tribological tests. The surface roughness of the ball measured by means of AFM technique was 18 ± 4 nm rms. All experiments were conducted at ambient conditions. Low velocities of the moving counterpart enabled measurement of the adhesive component of frictional interactions. The relative error for the friction and wear tests was below 5%. The detailed parameters of the microtribometer T-23 are shown in Table 2.

2.7. Wear scar analysis

An optical microscope operating at 80xmagnification was used to observe the sample surface before and after tribological tests. This analysis consisted of measurements of the width of all visible wear scars after microtribological tests. The scar width was calculated as an arithmetical average of at least three width measurements for one scar being the result of friction at given normal load. Measurement was performed for three independent scars appeared after tests at the same load.

3. Results and discussion

3.1. Nanoparticles characterization

Fig. 2 presents HR-TEM of zirconia nanoparticles. The ZrO_2 particles are agglomerated, crystalline (most probably single-crystalline without any defects such as twinning

Table 2
Detailed parameters of frictional tests performed on the microtribometer.

Counterpart:	TZP (ZrO_2/3%Y_2O_3) ball $d=5$ mm, surface roughness: 18 ± 4 nm rms.
Velocity:	25 mm min^{-1}
Frictional distance:	10 mm
Normal load:	80 mN
Number of cycles:	12, 24, 48 and 100 cycles (one cycle consisted of moving sample up and down at the same normal load on the same path)

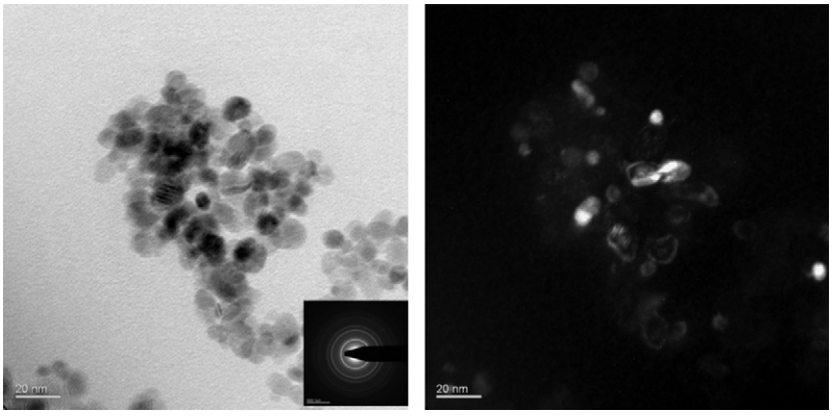

Fig. 2. Bright field of the differently oriented and crystalline ZrO_2 particles. The darker and brighter features visible originate from overlapping of the individual crystallites. The particles are rather agglomerated. The inset scale bar on the left image is 5000 1/μm.

or stacking faults), their size varies from about 5 nm to 20 nm. They have a rather spherical shape. From the crystallographic point of view, they have a cubic structure as confirmed by the diffraction pattern.

3.2. Surface topography and thickness of coatings

Figs. (3) and (4) present AFM and SEM images of the surface topography and the surface profile of the titania coatings. It was found that TiO_2 coatings annealed at 500 °C and 1000 °C were smooth, homogenous, without any cracks over a large scan areas. The temperature of annealing (500 °C and 1000 °C) do not affect the uniformity of the coating but influences its roughness. Average roughness (R_a) for titania coating increased from 0.4 nm to 1.9 nm for annealing at 500 °C and 1000 °C, respectively.

The surface topographies and the surface profiles of nanocomposites annealed at these temperatures consisting of titania with zirconia nanoparticle agglomerates with average height about 1.2 μm are visible in Figs. (5) and (9). These agglomerates are strongly bonded to the surface. The stress induced during sliding neither separate them from the surface nor decompose individual agglomerates under applied normal load. The roughness of nanocomposite coatings annealed at 500 °C is high–R_a (500 °C) = 264 nm. In the case of nanocomposite coatings, an increase of the number of drops from 3 to 6 considerably changes the surface topography. An increase of the size of agglomerates up to 2.5 μm and the surface roughness up to R_a (500 °C) = 520 nm was observed Fig. 7. The roughness of the coating prepared by deposition of 10 drops was not possible to measure using the AFM because of the scanner limit in the z-range. The average surface roughness for coating with nanoparticles prepared by deposition of 3 drops annealed at 500 °C and 1000 °C are similar: R_a (500 °C) = 264 nm (Fig. 5) and R_a (1000 °C) = 234 nm (Fig. 9), respectively.

Changes in surface topography are also visible in SEM images. Structures observed using SEM are very similar to these observed by AFM. The surface of nanocomposite coatings annealed at 500 °C prepared by deposition of 3 drops of sol is shown in Fig. 6. As the number of deposited drops increases the surface topography changes. Meander-like structures appear instead of separated islands of agglomerates Fig. 8.

The thickness of the titania coating annealed at 500 °C measured by ellipsometry was 66 nm and 107 nm deposited by 3 and 6 drops respectively. The thickness of the native silicon oxide covering silicon wafer was 2.5 nm. The thickness of the nanocomposite coatings was not possible to measure by ellipsometry due to the high light scattering from its rough surface. The thickness of the coatings annealed at 1000 °C was not measured. However it should be comparable or less to the thickness obtained for coatings annealed at 500 °C because of the materials shrinkage.

3.3. Coefficient of friction

Fig. 10 shows coefficient of friction (CoF) for titania coatings and composite coatings containing zirconia nanoparticles. The CoF was estimated as a ratio of measured friction force to the applied normal load recorded during

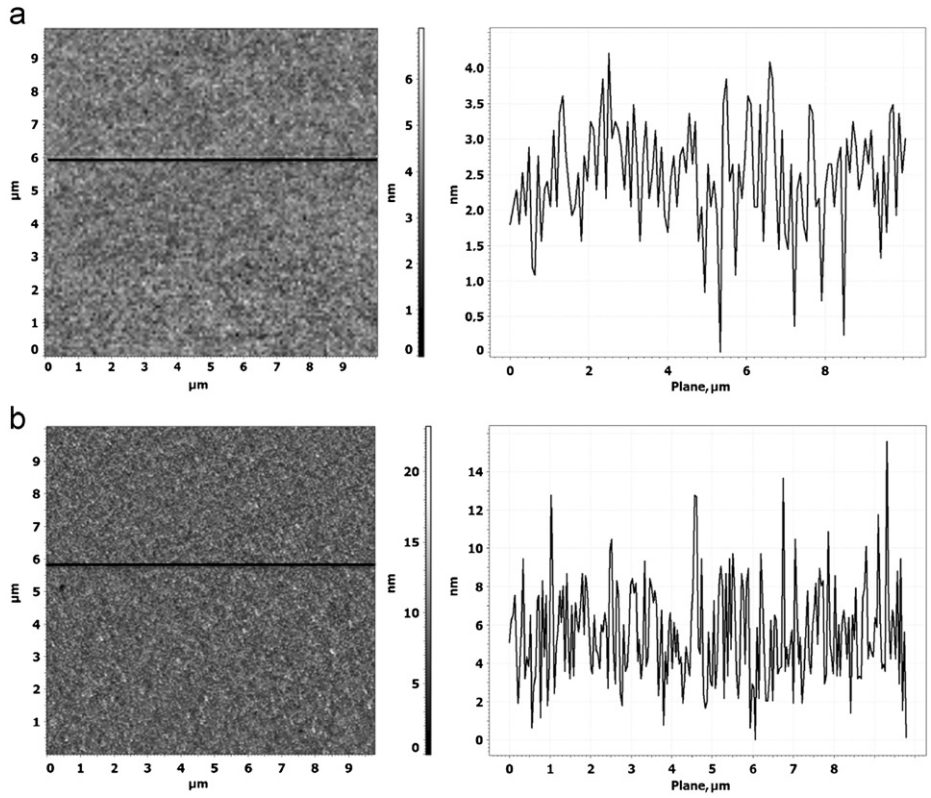

Fig. 3. AFM images of the surface topography with a cross section of titania coating annealed at 500 °C (a) and 1000 °C (b). (a) Titania coatings annealed at 500 °C (R_a=0.4 nm) and (b) titania coatings annealed at 1000 °C (R_a=1.9 nm).

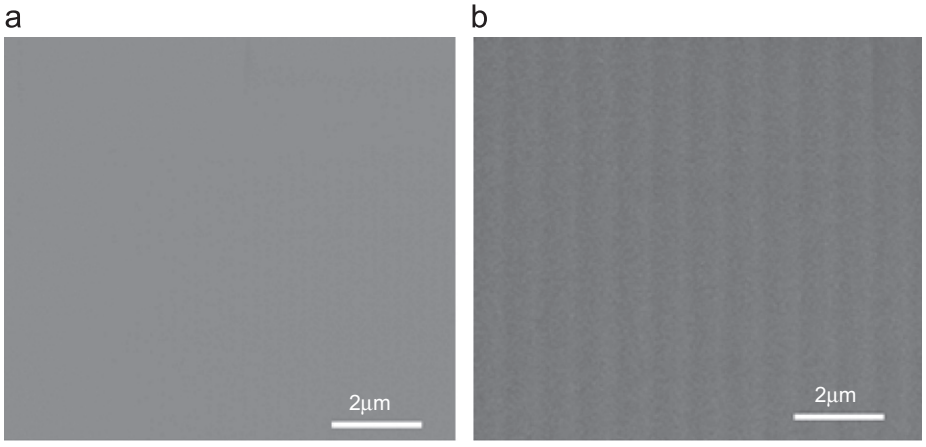

Fig. 4. SEM images of TiO_2 coating annealed at 500 °C (a) and 1000 °C (b).

tribological tests performed on the microtribometer. As expected, nanocomposites exhibit lower coefficient of friction as compared to the titania coating annealed at given temperature. The most significant reduction of the CoF (ca. 40%) was observed passing from purely titania to zirconia/titania nanocomposite coatings deposited by 3 drops annealed at 500 °C. In this case also the slight reduction of wear was observed.

An increase of the annealing temperature from 500 °C to 1000 °C causes the important reduction of the CoF from 0.62 to 0.30 for titania coatings Table 3. For nanocomposite coatings an increase of the temperature from 500 °C to 1000 °C causes the following reduction of the CoF values: 0.37–0.23; 0.42–0.20; and from 0.56 to 0.21 respectively for nanocomposites prepared using 3-, 6- and 10-drops deposition Table 3. The mechanism of the CoF lowering lies in the phase transition. It is known, that titania annealed at 500 °C exhibit anatase structure while titania heat-treated at 1000 °C exhibit rutile phase [19,20]. The hardness of anatase and rutile in Vickers scale equals respectively VHN_{100} = 616–698 kg/mm^2 and VHN_{100} = 894–974 kg/mm^2. Harder coating undergoes lower wear causing reduction of the CoF.

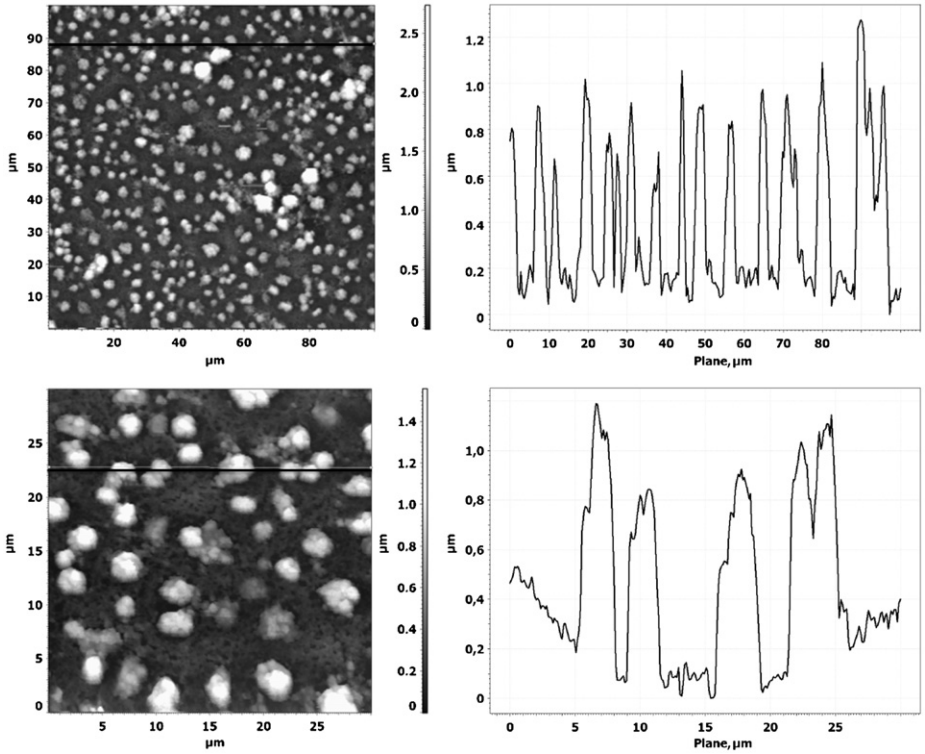

Fig. 5. AFM images of the surface topography with a cross section of 3-droped nanocomposite thin titania coating containing zirconia nanoparticles annealed at 500 °C (R_a=264 nm).

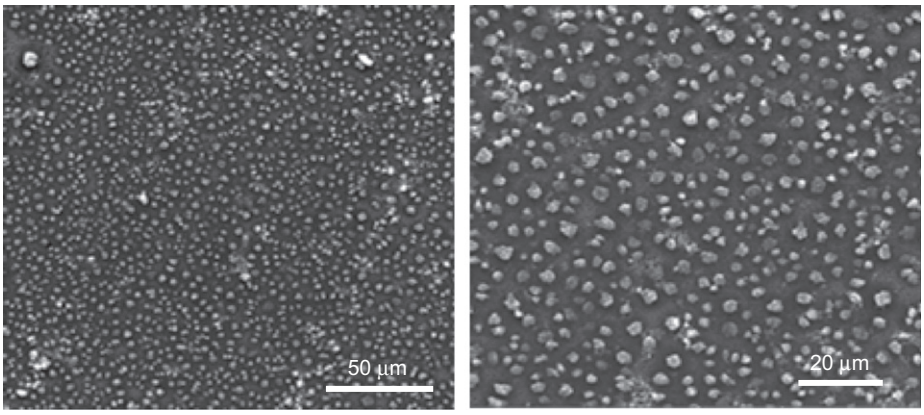

Fig. 6. SEM images of 3 drops ZrO_2/TiO_2 nanocomposite coatings annealed at 500 °C.

Considering the nanocomposite coatings deposited by 3 drops, agglomerate-like structure play an important role in reducing friction due to reduction of the contact area between sample and the counterpart. In our opinion, the mechanism of CoF reduction is based on the lower adhesion forces due to the presence large objects on the surface (asperities) reducing the real area of contact. Besides phase transition upon heating, the appearance of the hard zirconia nanoparticles additionally enhance the wear performance of the nanocomposite. Comparing CoF values for coatings annealed at 500 °C and 1000 °C it can be noticed that the direction of changing of the CoF follows changes in wear. CoF and wear follow the same trend. It means that there is strong dependence of the CoF on wear. An increase in wear causes larger CoF due to the presence of wear debris. It is very well visible for coating heat-treated at 500 °C (Fig. 10). Coefficients of frictions pursue the trend of changes in wear. For coatings annealed at 500 °C the highest CoF was recorded for 10 drops nanocomposite coating. In this case the zirconia nanoparticles were weakly bounded to the coating due to the weak consolidation of the film. Large surface roughness combined with high wear causes considerably increase in CoF. In contrary to coatings heated at 500 C, purely titania and zirconia/titania nanocomposite coatings heat-treated at 1000 °C exhibit stable and low CoF and minimal wear values. This concern also coatings deposited

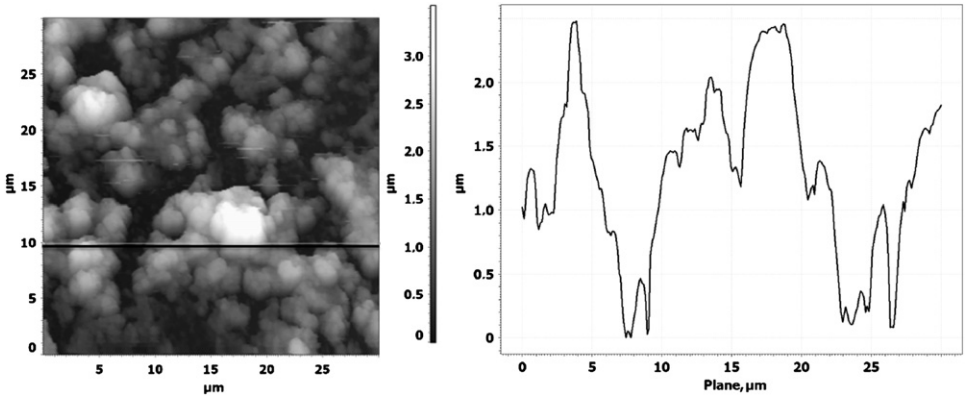

Fig. 7. AFM images of the surface topography with a cross section of 6-droped nanocomposite thin titania coating containing zirconia nanoparticles annealed at 500 °C (R_a=520 nm).

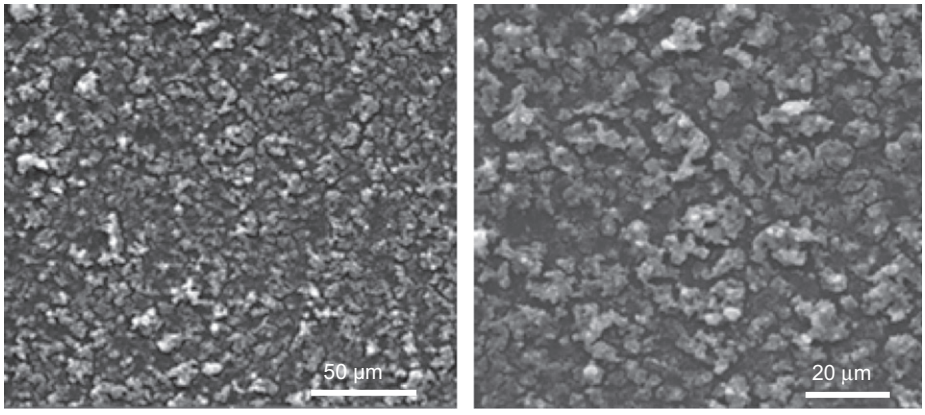

Fig. 8. SEM images of 6 drops ZrO_2/TiO_2 nanocomposite coatings annealed at 500 °C.

using 10 drops. In spite of high surface roughness, consolidated character of the film, combined with high hardness result in low wear and therefore in low CoF.

3.4. Wear tracks analysis

Wear tracks of titania coatings and titania nanocomposite coatings resulted from frictional tests were observed using optical microscopy as a function of the number of frictional cycles.

Titania coatings heated at 500 °C undergo visible wear already after 12 measurement cycles Figs. (11) and (13)a. Therefore longer tests consisting of 24, 48 and 100 cycles for this coating were not performed. The average width measured in optical microscope of the resulted scars has 61 μm Fig. 11. The depth of the scratch measured by AFM is 50 nm Fig. 13a. This is in good agreement with the coating thickness value obtained from elipsomery measurements (66 nm). Observed wear is caused by the differences in hardness between the coating and the counterbody. The soft titania coating is plastically deformed by hard zirconia ball as a result of strong penetration of the counterbody into the coating during sliding under the applied normal load. The mechanism of wear can be classified as scuffing additionally enhanced by the products of wear present in the frictional contact. These products can be adhered to the counterbody and tracked by it causing larger wear.

In the case of nanocomposites the addition of ZrO_2 nanoparticles into the titania coating considerably reduces the wear of the material Figs. (11) and (13)b. The width of the frictional traces is narrower than for pure titania coatings. Optical microscopy measurements revealed that the widths of the were tracks were 45 μm and 56 μm for coatings deposited using 3 and 6 drops annealed at 500 °C, respectively. However, for coatings deposited using 10 drops of sol, heated at 500 °C, an increase of the wear was observed. This is caused by the weak adhesion of the nanoparticles to the coating and scaling off the material due to its excess. Free nanoparticles behave as additional abrasive particles causing larger wear. It means that the adhesion of the nanoparticles in the coating also depends on the amount of the deposited material. Tribological tests reveled the lowest adhesion of nanoparticles for 10 drops nanocomposite.

An increase of the temperature of annealing from 500 °C to 1000 °C causes an enhancement of the antiwear

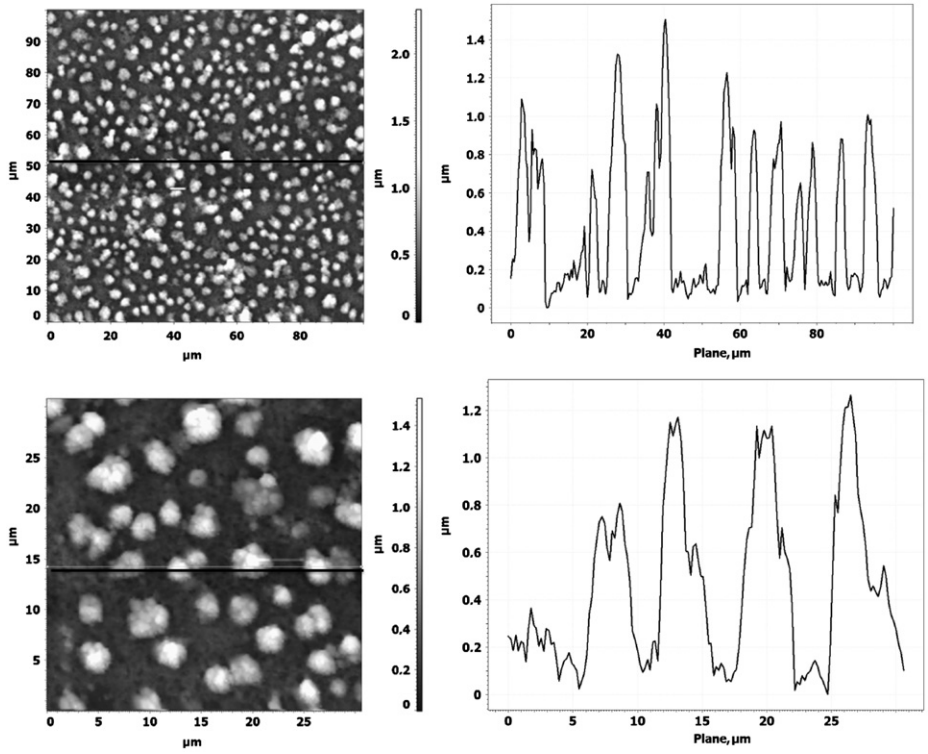

Fig. 9. AFM images of the surface topography with a cross section for 3-droped nanocomposite thin titania coating containing zirconia nanoparticles annealed at 1000 °C (R_a=234 nm).

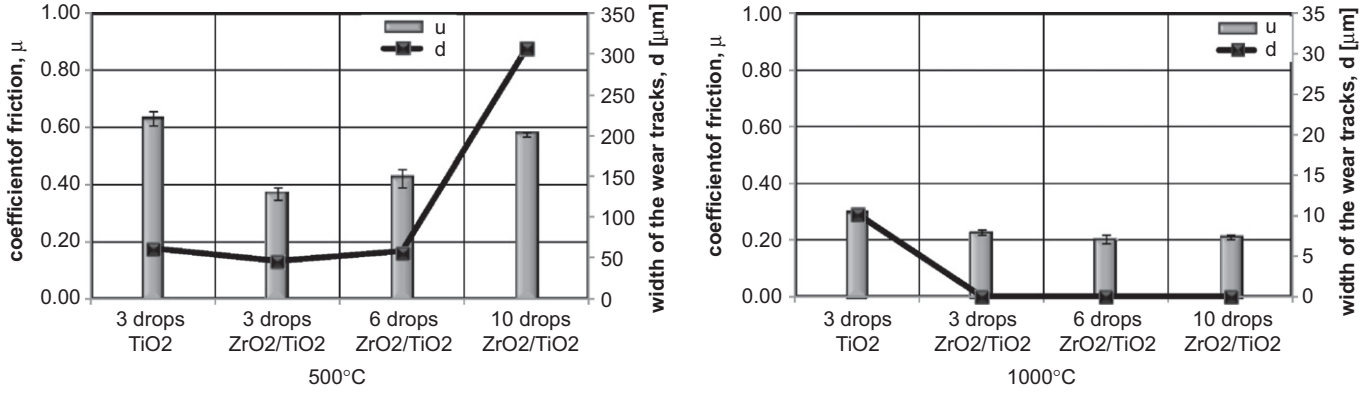

Fig. 10. Dependence of the coefficient friction (bars) and the wear scar width after 12 cycles (points with solid lines) on the number of deposited drops in preparation process for coatings heated at 500 °C and 1000 °C.

Table 3
Comparison of the coefficients of friction (CoF) for titania coatings and composite titania coatings containing zirconia nanoparticles.

Annealing temperature	500 °C		1000 °C	
	CoF	Thickness (nm)	CoF	Thickness (nm)
3 drops titania coating	0.62 ± 0.02	66	0.30 ± 0.01	–
6 drops titania coating	0.62 ± 0.02	107	0.30 ± 0.01	–
10 drops titania coating	0.62 ± 0.02	–	0.31 ± 0.01	–
3 drops composite coating	0.37 ± 0.01	–	0.23 ± 0.01	–
6 drops composite coating	0.42 ± 0.02	–	0.20 ± 0.01	–
10 drops composite coating	0.56 ± 0.02	–	0.21 ± 0.01	–

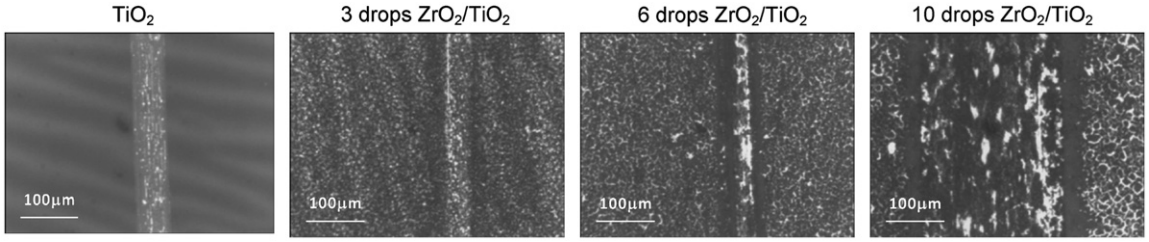

Fig. 11. Wear scars visible on the surface of the nanocomposite coatings ZrO_2/TiO_2 heated at 500 °C after 12 measurement cycles. Images obtained in optical microscope.

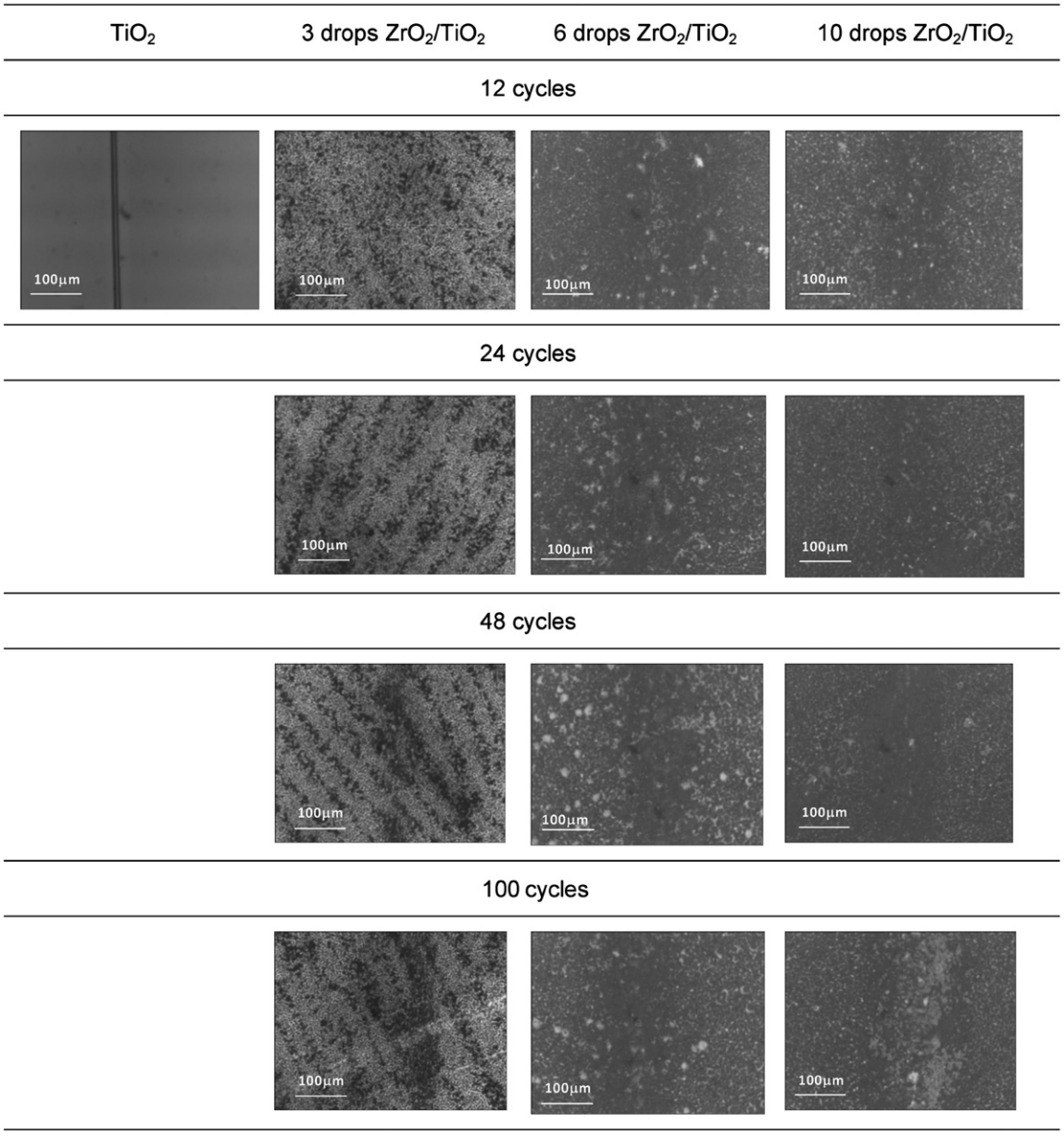

Fig. 12. Wear scars visible on the surface of titania (TiO_2) and nanocpomposite (ZrO_2/TiO_2) coatings heated at 1000 °C for various number of measurement cycles. Images obtained in optical microscope.

properties of the coating due to the phase transition of anatase to rutile [19,20]. Since rutile exhibit higher hardness than anatase, coatings heat treated at 1000 °C are more resistant to wear (Fig. 12). For coating annealed at 1000 °C the wear track having 10 μm was observed using optical microscopy (Fig. 12).

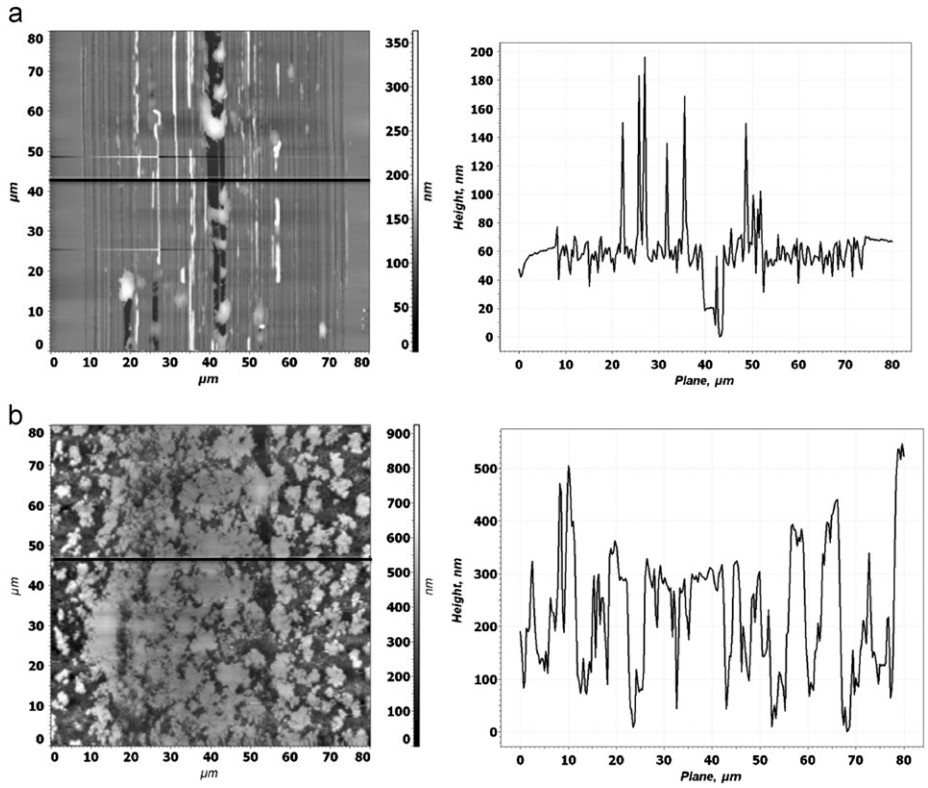

Fig. 13. AFM images and cross sections of the wear tracks for TiO_2 coating annealed at 500 °C after tribological tests (a), and for 3 drops ZrO_2/TiO_2 nanocomposite coatings annealed at 500 °C (b), (normal load of 80 mN, 12 cycles).

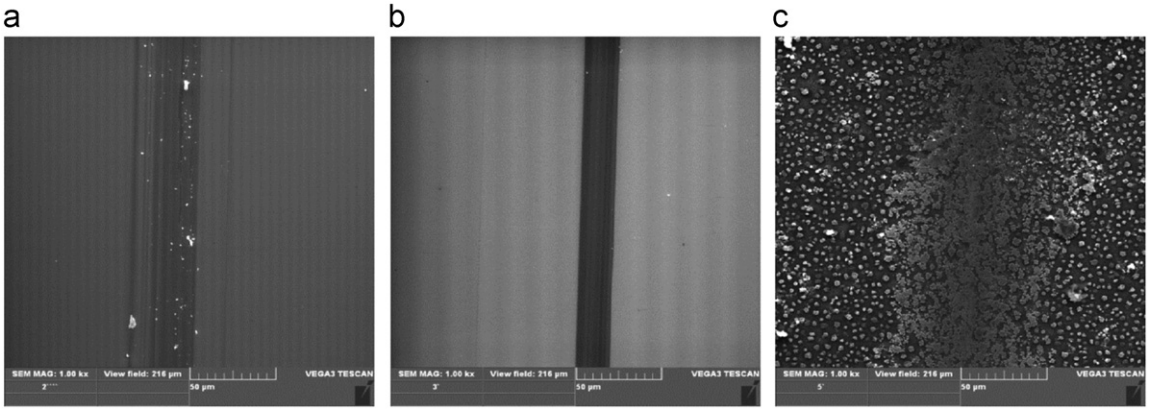

Fig. 14. SEM images of the wear tracks after tribological tests: TiO_2 coating annealed at 500 °C (a) TiO_2 coating annealed at 1000 °C (b), 3 drops ZrO_2/TiO_2 nanocomposite coatings annealed at 500 °C (normal load of 80 mN, 12 cycles).

Upon the standard frictional tests consisting of 12 measurement cycles for composites containing zirconia nanoparticles annealed at 1000 °C (3 drops deposition) the abrasive wear was not observed Fig. 12. Some tiny traces of tribological experiments detectable in AFM measurements appeared on the surface of the nanocomposite annealed at 1000 °C after 48 frictional cycles carried out at 80 mN normal load Fig. 15a. It was found, on the basis of AFM observations, that after frictional tests the surface of nanocomposite coatings undergo plastic deformation instead of abrasive wear. An increase of the frictional cycles up to 100 did not result in degradation of the nanocomposite coating but rather in its plastic deformation Figs. (14) and (15)b. Neither the extraction of the zirconia nanoparticles form the titania coating under friction was observed nor the abrasive wear was detected. Strong interactions between zirconia nanoparticles forming agglomerate structures effectively prevent its removing form the frictional contact under external load. In this way agglomerate-like structures build of closely packed zirconia nanoparticles additionally reinforced by thin titania layers

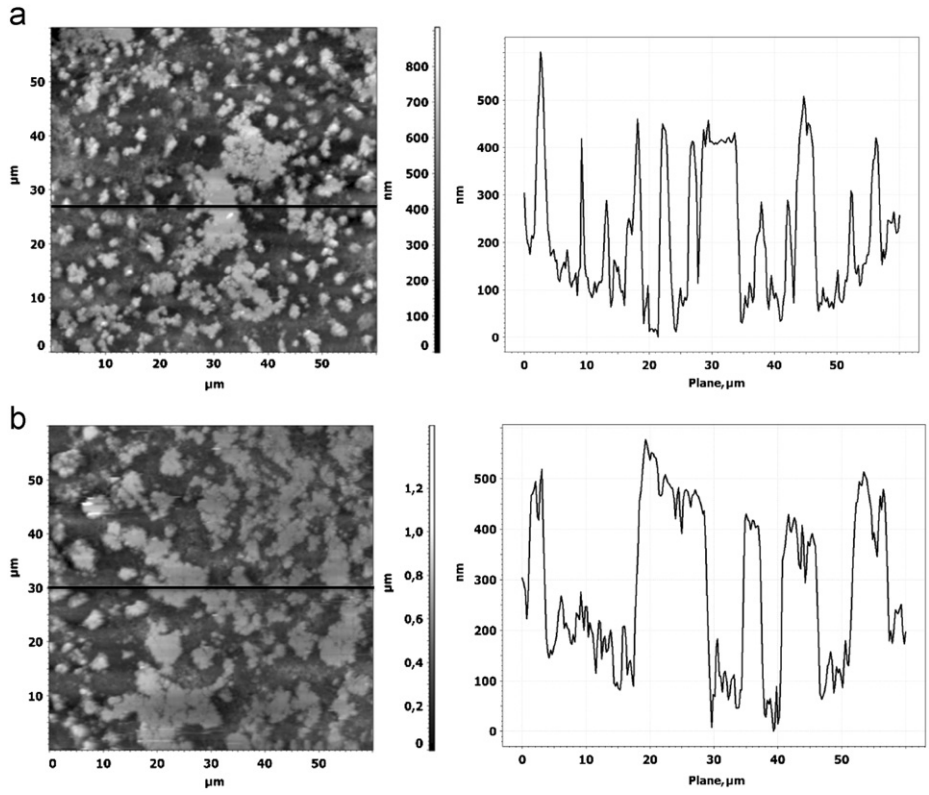

Fig. 15. AFM images and cross sections of the wear tracks for 3 drops ZrO_2/TiO_2 nanocomposite annealed at 1000 °C after tribological tests at normal load of 80 mN after 48 cycles (a) and 100 cycles (b).

filling spaces between nanoparticles effectively protect the coating against wear.

In the case of 6 or 10 drop nanocomposite coatings the trace after frictional test is visible Fig. 12. However, the removing of the material was not observed. As revealed AFM microscopy measurements, instead of ploughing (typical for titania coatings without nanoparticles), a polishing of the coating with microscratching accompanied by squeezing of the agglomerates took place Figs. 14–16. After frictional tests agglomerates are still strongly adhered to the coatings and quite homogenously distributed over the surface. Their height reaches 0.6 µm. The average surface roughness R_a after tribological tests is also high: 102 nm and 110 nm for 3 drops nanocomposites annealed at 500 °C and 1000 °C respectively. Such type of topography reduces the real contact area between the surfaces of nanocomposite coating and the counterbody resulting in lowering of the adhesion. In this model, the shearing forces needed to break adhesion contacts are low, which result in lowering of the wear.

After tribological tests the counterpart was also analyzing in optical microscope. Since experiments were conducted under relatively low loads, no detectable traces of wear was found on zirconia ball.

Collected results indicate, that the tribological properties of the investigated nanocomposites are related to the structure and surface topography of the coatings. The structural properties of the interface determine the behavior of

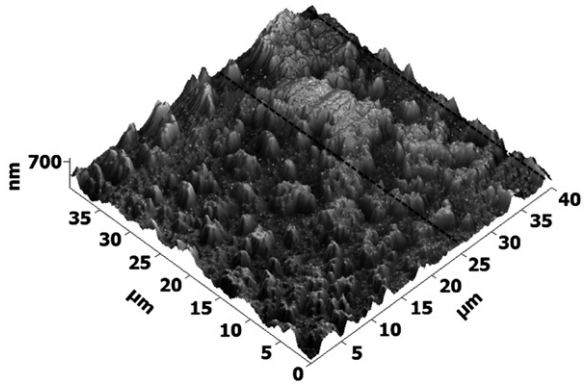

Fig. 16. 3D AFM image of the wear tracks for 3 drops ZrO_2/TiO_2 nanocomposite annealed at 1000 °C after tribological tests at normal load of 80 mN after 100 cycles.

frictional contact. The common mechanical properties have secondary influence. Analyzing the mechanism of the wear it is clear that adhesive forces between the coating and counterbody surfaces are lower than cohesive forces existing within the coating and the adhesion of the coating to the substrate. Island-like structures, existing on the surface, lower the real area of contact and affect the obtained mechanism of wear. Lowering of friction and wear result also from the presence of hard ceramic nanoparticles in relatively soft titania matrix. An increase of hardness especially for coatings annealed at 1000 °C causes lower wear and reduction of friction. In our

opinion changes in chemical composition of contacting asperities passing from titania/zirconia to nanocomposite titania/zirconia tribological coupling are less important.

4. Conclusions

The titania coatings and the composite coatings containing zirconia nanoparticles were prepared by the sol–gel spin-coating method using titanium alkoxide as titania precursor. It was shown that composite coatings containing ZrO_2 nanoparticles exhibit enhanced frictional behavior as compared to titania coatings without nanoparticles. The improved friction behavior of the modified surfaces was attributed to their lower intrinsic adhesion and reduced real area of contact. In performed experiments both the size and shape factors of the patterns (agglomerate-like structures), are decisive in determining the contact area. These factors together contribute to the reduction of their friction values as compared to titania coating.

The composite coatings containing ZrO_2 nanoparticles showed improved performance in scratch resistance as compared to that of bare titania coatings. This improvement in scratch resistance is attributed to the arrangement of hard of ZrO_2 nanoparticles, in the form of agglomerates, strongly adhered to the surface of titania coatings. In the case of the nanocomposites heat-treated at 500 °C the processes of wear are associated to the loss of mass visible as ploughing or shearing of the asperities. For nanocomposites heat-treated at 1000 °C instead of the removing the material from the coating, the geometry of existing agglomerates is altered due to their pressing and polishing.

In general the following conclusions can be drown from performed tribological investigations:

1. Nanocomposites exhibited lower coefficient of friction as compared to bare titania coating. The lower friction of nanocomposite coatings is due to lower adhesion and reduced contact area (physical reduction through geometry).
2. Prepared nanocomposites exhibited better wear resistance when compared to bare titania coatings.
3. The presence of hard nanoparticles can considerably enhance the wear resistance of the coating. Larger hardness of nanometer-sized structures is due to their large surface-area-to-volume ratio and their nearly defect-free nature.
4. Behavior of frictional contact is also influenced by the modification of the tribological coupling from ZrO_2/TiO_2 to ZrO_2/ZrO_2 on the top of the asperities. In our opinion this effect has lower influence than topography changes.
5. Changing the surface topography by surface texturing or building elements reducing the area of contact can be effective way in lowering of wear and friction in micro-, nano- scale.

Acknowledgments

Special thanks we address to Magdalena Parlińska-Wojtan from EMPA Institute (Switzerland) for TEM measurements and helpful discussions. This work was supported by the Ministry of Science and Higher Education of Poland. Grant nos.: N N507 401039 and N N507 497538.

Appendix A. Supporting information

Supplementary data associated with this article can be found in the online version at http://dx.doi.org/10.1016/j.ceramint.2012.07.034.

References

[1] T.A. Blanchet, S.S. Kandanur, L.S. Schadler, Coupled effect of filler content and countersurface roughness on ptfe nanocomposite wear resistance, Tribology Letters 40 (2010) 11–21.
[2] L. Chang, Z. Zhang, L. Ye, K. Friedrich, Tribological properties of high temperature resistant polymer composites with fine particles, Tribology International 40 (2007) 1170–1178.
[3] I. Piwoński, K. Soliwoda, The effect of ceramic nanoparticles on tribological properties of alumina sol–gel thin coatings, Ceramics International 36 (2010) 47–54.
[4] M. Madej, D. Ozimina, Electroless Ni–P–Al_2O_3 composite coatings, Kovove Materialy 44 (2006) 290–296.
[5] D.P. Singh, A.K. Singh, O.N. Srivastava, Formation and size dependence of germanium nanoparticles at different helium pressures, Journal of Nanoscience and Nanotechnology 3 (2003) 545–548.
[6] Y. Huh, M.L.H. Green, Y.H. Kim, J.Y. Lee, C.J. Lee, Control of carbon nanotube growth using cobalt nanoparticles as catalyst, Applied Surfrace Science 249 (2005) 145–150.
[7] T.S. Yoon, J. Oh, S.H. Park, V. Kim, B.G. Jung, S.H. Min, J. Park, T. Hyeon, K.B. Kim, Single and multiple-step dip-coating of colloidal maghemite (γ-Fe_2O_3) nanoparticles onto Si, Si_3N_4, and SiO_2 substrates, Advanced Functional Materials 14 (2004) 1062–1068.
[8] F.K. Liu, Y.Ch. Changb, F.H. Koa, T.Ch. Chub, B.T. Daia, Rapid fabrication of high quality self-assembled nanometer gold particles by spin-coating method, Microelectronic Engineering 67–68 (2003) 702–709.
[9] M. Altissimo, F. Romanato, L. Vaccari, L. Businaro, D.A. Cojoc, B. Kaulich, S. Cabrini, E. Di Fabrizio, X-ray lithography fabrication of a zone plate for X-rays in the range from 15 to 30 keV, Microelectronic Engineering 61-62 (2002) 173–177.
[10] R. Murillo, H.A. van Wolferen, L. Abelmann, J.C. Lodder, Fabrication of patterned magnetic nanodots by laser interference lithography, Microelectronic Engineering 78–79 (2005) 260–265.
[11] Y. Kono, A. Sekiguchi, Y. Hirai, S. Arasaki, K. Hattori, Study on nano imprint lithography by the pre-exposure process (PEP), Proceedings of SPIE 5753 (2005) 912–925.
[12] R.P. Nair, M. Zou, Surface-nano-texturing by aluminum-induced crystallization of amorphous silicon, Surface and Coatings Technology 203 (2008) 675–679.
[13] M. Shafiei, A.T. Alpas, Nanocrystalline nickel films with lotus leaf texture for superhydrophobic and low friction surfaces, Applied Surface Science 256 (2009) 710–719.
[14] T.S. Kustandi, J.H. Choo, H.Y. Low, S.K. Sinha, Texturing of UHMWPE surface via NIL for low friction and wear properties, Journal of Physics D: Applied Physics 43 (2010) 015301 (6pp).

[15] A. Määttä, P. Vuoristo, T. Mäntylä, Friction and adhesion of stainless steel strip against tool steels in unlubricated sliding with high contact load, Tribology International 34 (2001) 779–786.
[16] T. Kratschmer, C.G. Aneziris, P. Gruner, Mechanical properties of flame sprayed free-standing coatings, Ceramics International 37 (2011) 2727–2735.
[17] Y. Chen, J. Zhou, W. Liu, Preparation and tribological properties of TiO_2–ZrO_2 thin films, Chinese Journal of Materials Research/Cailiao Yanjiu Xuebao 16 (2002) 279–284.
[18] K. Kato, K. Adachi, Wear of advanced ceramics, Wear 253 (2002) 1097–1104.
[19] E. Traversa, G. Gnappi, A. Montenero, G. Gusmano, Ceramic thin films by sol–gel processing as novel materials for integrated sensor, Sensors and Actuators B 31 (1996) 59–70.
[20] Ch.H. Kwon, J.H. Kim, J.S. Junge, H. Shin, K.H. Yoon, Preparation and characterization of TiO2–SiO2 nano-composite thin films, Ceramics International 29 (2003) 851–856.